


Effective-mode analysis of the dynamics of weakly bound molecular systems by an example of hydrogen-bonded water clusters

E. D. Belega^{1,*}, M. N. Zakirov², A. I. Chulichkov³, D. N. Trubnikov¹ and Yu. V. Novakovskaya^{1,†}

¹*Department of Chemistry, M. V. Lomonosov Moscow State University, Leninskie Gory 1/3, Moscow 119991, Russia*

²*A. M. Obukhov Institute of Atmospheric Physics, Russian Academy of Sciences, Moscow 119017, Russia*

³*Department of Physics, M. V. Lomonosov Moscow State University, Leninskie Gory 1/2, Moscow 119991, Russia*

 (Received 11 November 2022; revised 13 January 2023; accepted 13 February 2023; published 14 March 2023)

A method for the analysis of internal dynamics of nonlinear weakly bound polymolecular systems based on the effective-mode approach is proposed. The method enables one to estimate the number of the governing collective degrees of freedom of the system of interest at a preset accuracy under particular conditions and analyze the character of the modes depending on the activation energy of the system and the duration of its dynamic propagation, which provides qualitative and quantitative information about the coupling of diverse motions and the respective energy redistribution. The method is applied to the analysis of the dynamics of small water clusters stabilized by hydrogen bonds, which are unique spectacular examples of the systems with a pronounced coupling between the intramolecular and substantially delocalized intermolecular oscillations. The dynamic trajectories were generated in the adiabatic approximation at the Born-Oppenheimer level with the use of the quantum chemical description of selected clusters at the MP2/6–311++G(*d*, *p*) level. The initial conditions corresponded to different variants of the excitation of low-frequency normal modes, and the dynamic runs were carried out at a time step of 0.5 fs and the whole duration of 50 to 100 ps. Different prevailing characters of the cluster dynamics were identified depending on the molecular size, the total activation energy, and the mean potential-energy-increment to kinetic-energy-increment ratio, from an efficient accumulation of the excess kinetic energy on the effective modes of the cluster to the dissociation of the cluster into constituting fragments. The signs of the corresponding processes in the overlap matrices of the effective-mode vectors, kinetic-energy distribution over the modes, and the correlation between the number of the modes and the mean kinetic energy of the cluster are distinguished.

DOI: [10.1103/PhysRevA.107.032812](https://doi.org/10.1103/PhysRevA.107.032812)

I. INTRODUCTION

Fundamental problems people face when describing finite-size weakly bound atomic and molecular clusters are related to their dynamic and thermodynamic properties [1]. Estimation of the dynamic characteristics of a cluster involves analyzing those phase-space domains where the trajectory of the system is chiefly localized, searching for the parameters that control the system dynamics, and whenever possible distinguishing characteristic collective motions of the particles that constitute the system of interest and their spectral fingerprints.

Interpreting the inner dynamics of weakly bound atomic and molecular clusters meets certain difficulties. The normal-mode approach is typically valid in the energy ranges that are not far from the energies of the equilibrium cluster structures and within the configuration space domains in the vicinity of these structures, because the strong nonlinearity of the system dynamics results in a substantial mixing of all basic types of motions.

Historically, the first results concerning the dynamics of weakly bound atomic clusters were obtained for nonrotating

clusters of noble gas atoms [2]. In the case of a rotating triatomic Ar₃ cluster, the phase-space regions with the predominant regular and chaotic dynamics were studied depending on the total energy and total angular momentum of the system [3]. A strong coupling between the rotational and vibrational states within the chaotic dynamics region was noticed.

In the case of more strongly bound molecular clusters, such as those stabilized by hydrogen bonds (H-bonds), the dynamics of relatively small- and medium-sized clusters composed of water molecules [(H₂O)_{*n*} with *n* = 5–20] was studied previously and aimed at identifying the most probable configurations of the H-bond networks depending on the total energy of the system or its temperature chiefly with the use of empirical potentials [4–16].

Insofar as the interactions between particles in such clusters are determined by nonquadratic potentials, the character of the dynamic propagation of the system can and should be governed by a varying number of modes, which are essentially collective degrees of freedom. Even the seemingly localized high-frequency intramolecular vibrational motions can be substantially coupled both to each other when the oscillating fragments belong to the neighboring H-bonded molecules and to the lower-frequency vibrations due to the multiplicity of the frequencies (akin resonances in individual

*Corresponding author: EDBelega@gmail.com

†Corresponding author: jvn@phys.chem.msu.ru

molecules between stretching and twice as excited deformation oscillations). Such interactions should become more noticeable with an increase in the excitation energy and govern the energy redistribution among various combinations of basic vibrational motions. The signs and criteria of such redistribution are important not only in view of the particular structure reorganization of the H-bonded species, which is related particularly to their reactivity and absorbance of radiation, but also for estimating the thermodynamic characteristics of the systems as well. Thermodynamic parameters that are used in the theory of clusters, namely, entropy, temperature, and specific heat capacitance, are adapted from the classical thermodynamics, and their changes enable one to identify phase transitions. For example, the cluster temperature, which is treated as an inner system parameter, can be defined as the kinetic energy normalized to the number of vibrational degrees of freedom [2,17].

Because of the strong coupling of all the motion kinds in weakly bound systems, an approach based on the effective-mode analysis (EMA) was proposed for describing the dynamics of clusters, originally atomic ones. The method is similar to the biorthogonal decomposition method described in [18] and the Karhunen-Löve decomposition method described, e.g., in [19,20]. It is worth noting that EMA, biorthogonal decomposition, and Karhunen-Löve decomposition can be treated as modifications of the principal component analysis (PCA) proposed by Pearson in 1901 [21] and efficiently implemented in diverse fields [22]. The essence of PCA is in decreasing the dimensionality of data so that the maximum possible amount of information is retained. That is why the PCA method is applied to study collective motion in macromolecules, where the number of atoms moving in a concerted way is very large. The method was applied as quasiharmonic analysis for displaying the large-scale low-frequency modes of proteins [23] and to estimating the configuration entropy of macromolecules [24]. The PCA is also typically used in determining the vibrational frequencies of small molecules. For example, the principal mode analysis (PMA) was applied [25] to the analysis of intra- and intermolecular vibrations of a water monomer, a water dimer, and a water molecule in liquid water. The criteria for using the PMA method for assessing the frequencies of oscillations in molecular systems are discussed in [26]. It is argued that the method can provide accurate frequencies when the interaction potential of the particles in a molecule is harmonic and the kinetic energy is evenly distributed over all modes. The question about the accuracy of calculated frequencies is also discussed in [27] where the frequencies of intramolecular motions in a water molecule are estimated with the use of two methods, namely, the normal-coordinate approximation and the PMA. The results show how to obtain characteristic frequencies for each mode without invoking an assumption about the energy equipartition. To decompose vibrational spectra of molecular systems into modes, a variation of the effective-mode method was suggested in [28]. Here, the effective normal-mode method was based on a localization criterion for the Fourier-transform velocity time-correlation functions of the effective modes. It should be noted that the aforementioned works dealing with the application of the PCA or its variations to vibrational spectroscopy problems are usually restricted to

the classical descriptions of the nuclei interactions. In [29] the authors extended the PCA method to quantum trajectories to compute the infrared spectra of several polycyclic aromatic hydrocarbon molecules, such as naphthalene ($C_{10}H_8$) and pyrene ($C_{16}H_{10}$). The authors also suggested a new approach called the self-consistent phonons (SCP) method. The latter one is a practical approach for computing structural and dynamic properties of a general quantum or classical many-body system while incorporating anharmonicity. The SCP method was later applied to classical Lennard-Jones clusters [30].

Previously, we have used the effective-mode method as a modification of PCA for the analysis of the internal dynamics of a triatomic cluster composed of argon atoms to visualize the motion of the cluster as a whole [31], distinguish the phase-space regions with the predominant regular and chaotic dynamics depending on the total angular momentum of the rotating system [32–34], as well as separate the vibrational and rotational components in the cluster dynamics [33]. In the case of molecular clusters, the analysis of the effective phase space becomes more complex because molecules involve atoms of different masses, and there are intra- and intermolecular interactions and effective motions of diverse kinds.

As regards the objects of investigation in this paper, they deserve special attention. An interest in the dynamic characteristics of the clusters composed of water molecules is related to a number of fundamental problems. One of them can be formulated as follows: what are the key characteristics of the H-bond network in such species, which are intermediate between individual molecules and extended H-bonded fragments in the bulk of a condensed phase [10,13,14,16,35]? The characteristics include not only the static parameters of the ordered arrangement of molecules, but also the dynamic features of their collective motions, which are crucial for their response to external effects; the stronger the impact, the more pronounced the local reorganization, which can later on spread over and touch the neighboring fragments of larger species. For example, molecular clusters are interesting and informative species for studying the phase transitions in weakly bound molecular systems [36]. In this paper, the effective-mode analysis is applied to the dynamics of small water clusters composed of three to five molecules. Note that the method of effective modes used by us is not limited to relatively small variations of the stable cluster configurations, as required by the calculation of the autocorrelation function in the variant applied in [29], but allows us to study in detail the dynamics of clusters within broad configuration space domains.

The main object of this paper is to distinguish collective modes; estimate their composition with the use of the normal-mode basis; follow the changes in their character, number, and contribution to the dynamics of molecular water clusters depending on the excitation energy of the latter; and find out the quantitative indications of the particular structure reorganization. The paper has the following structure. The effective-mode approach is described in Sec. II. The results of the analysis applied to the internal dynamics of tri-, tetra-, and pentamolecular water clusters depending on the initial excitation energy are discussed in Sec. III. Here, the character of the activation and coupling of the modes depending on the total

energy of the system is considered and aimed at identifying general criteria of the character of cluster dynamics.

II. THE EFFECTIVE-MODE ANALYSIS IN THE CASE OF MOLECULAR SYSTEMS

For interpreting a cluster dynamics, it is expedient to represent a phase trajectory as a superposition of apparently independent contributions, each of which describes a particular collective motion of the atoms that constitute the whole system of interest. For example, the dynamics of an N -particle system close to its equilibrium configuration, which corresponds to the potential-energy minimum in the vicinity of which the small-amplitude approximation for the nuclear motions is valid, can be considered as a linear combination of normal modes that are determined by independent equations [37] and represent collective harmonic motions with constant frequencies each.

However, when one turns to a cluster, the particles of which are bonded via more or less weak intermolecular contacts that are typically many-body in nature and characterized by anharmonic potentials, and especially when the kinetic energy of such a cluster increases, a linearized model is no longer a satisfactory approximation. In this paper, it is proposed to investigate the dynamics of systems with a strong nonlinearity based on the orthogonal components of the collective motions defined as follows. The time-averaged squared norm of the sum of m effective components should provide the most accurate approximation for the time-averaged physical property of the cluster, which can be given as a squared value of a Hermitian operator. For this purpose, an effective-mode analysis, which is a modification of the principal component analysis, is used.

The basic idea of the effective-mode analysis as applied to the dynamics of molecular clusters is the decomposition of the system dynamics in an n -dimensional phase space into orthogonal components ($m = 1, 2, \dots, n$) in such a way that a linear superposition of m components (effective modes) provides the best possible approximation of a quadratic function of the phase (position and/or momentum) coordinates.

Let us illustrate the effective-mode analysis by two examples. Let $\vec{x}(t) \in R^n$ ($t \in [0, T]$ is the time variable) be the phase trajectory of a system in R^n phase space. The problem is formulated as follows: the $\vec{x}(t)$ trajectory should be represented by an $\vec{x}(t) = \sum_{i=1}^n (\vec{x}(t), \vec{e}_i) \vec{e}_i$ expansion in the orthonormal $\{\vec{e}_i\} \subset R^n$ basis constructed in such a way that any m th partial sum

$$\vec{x}_m(t) = \sum_{i=1}^m (\vec{x}(t), \vec{e}_i) \vec{e}_i \quad (1)$$

approximates the $\vec{x}(t)$ trajectory in the time-averaged sense no worse than any m th partial sum $\vec{x}'_m(t) = \sum_{i=1}^m (\vec{x}(t), \vec{e}'_i) \vec{e}'_i$ of the expansion in any other orthonormal $\{\vec{e}'_i\} \subset R^n$ basis. Here, (\cdot, \cdot) denotes a scalar product in R^n , and the quality of the approximation is given by the time integral of the squared norm of the $\vec{x}(t)$ and $\vec{x}'_m(t)$ difference. Formally, the orthonormal $\{\vec{e}_i\}$ basis set can be obtained as the one that provides the greatest lower bound of the following functional over all the

orthonormal basis sets in R^n :

$$\inf_{\{\vec{e}'_i\} \subset R^n} \frac{1}{T} \int_0^T \left\| \vec{x}(t) - \sum_{i=1}^m (\vec{x}(t), \vec{e}'_i) \vec{e}'_i \right\|^2 dt.$$

The solution can be found in terms of the principal component analysis. To construct a $\{\vec{e}_i\}$ basis set with the specified extreme properties, one should solve the eigenvalue problem of a linear operator $X : R^n \rightarrow R^n$, the action of which on any vector $\vec{y} \in R^n$ is defined as

$$X\vec{y} = \frac{1}{T} \int_0^T \vec{x}(t)(\vec{x}(t), \vec{y}) dt. \quad (2)$$

The problem consists in determining the $\alpha_1^2, \alpha_2^2, \dots, \alpha_n^2$ eigenvalues and the corresponding $\vec{e}_1, \vec{e}_2, \dots, \vec{e}_n \in R^n$ eigenvectors, such that $X\vec{e}_i = \alpha_i^2 \vec{e}_i$, $i = 1, \dots, n$ (the α_i^2 eigenvalues are written as squared α_i real values to stress their non-negativity). If the eigenvalues are ordered as $\alpha_1^2 \geq \alpha_2^2 \geq \dots \geq \alpha_n^2 \geq 0$, the corresponding $\{\vec{e}_i\}$ eigenbasis is the one sought for. In this case, the following equalities are met:

$$\frac{1}{T} \int_0^T \left\| \sum_{i=1}^m (\vec{x}(t), \vec{e}_i) \vec{e}_i \right\|^2 dt = \sum_{i=1}^m \alpha_i^2, \quad (3)$$

$$\frac{1}{T} \int_0^T \left\| \vec{x}(t) - \sum_{i=1}^m (\vec{x}(t), \vec{e}_i) \vec{e}_i \right\|^2 dt = \sum_{i=m+1}^n \alpha_i^2, \quad m = 1, \dots, n. \quad (4)$$

When applied to a molecular cluster, Eq. (3) means that the m th partial sum (1) has a squared norm equal to the sum of the first m eigenvalues of the X operator, which is maximum among all m th partial sums, while Eq. (4) means that Eq. (1) approximates the $\vec{x}(t)$ ($t \in [0, T]$) trajectory with an accuracy which equals the sum of the last $(n-m)$ eigenvalues of the X operator that is minimum among all the corresponding partial sums. In practice, this makes it possible to distinguish a linear subspace of the lowest dimensionality, which contains the whole $\vec{x}(t)$ ($t \in [0, T]$) trajectory at the preset accuracy. At the same time, it is possible to estimate the fraction of the time-averaged squared norm of the $\vec{x}(t)$ trajectory in the m th partial sum (1), this fraction being $S_{X,m} = (\sum_{i=1}^m \alpha_i^2) / (\sum_{i=1}^n \alpha_i^2)$.

Thus, the properties of the extreme orthonormal $\{\vec{e}_i\}$ basis enable one to state that the whole $\vec{x}(t)$ ($t \in [0, T]$) trajectory can be represented by a sum of $(\vec{x}(t), \vec{e}_i) \vec{e}_i$ effective modes, the $\vec{e}_1, \vec{e}_2, \dots, \vec{e}_n$ vectors of which are mutually orthogonal collective motion modes in R^n , while the time dependent $(\vec{x}(t), \vec{e}_i(t))$ scalar products are the amplitudes of the effective modes. The mean squared value of the i th effective mode equals α_i^2 , $i = 1, \dots, n$, and its contribution to the time-averaged squared norm of the $\vec{x}(t)$ trajectory is $(\alpha_i^2) / (\sum_{i=1}^n \alpha_i^2)$.

Thus, the effective-mode analysis does not essentially differ from the principal component analysis. However, the variant proposed in this paper (which is on the whole similar to the one described in [29]) implies the possibility of using different metrics in the trajectory phase space, which enables one to decompose the system dynamics into modes, which meet extreme conditions not only in view of the squared norm

of the trajectory, but also some other dynamic characteristics, e.g., kinetic energy averaged over the trajectory. Additionally it provides the means for distinguishing the changes in the character of the governing effective modes with time depending on either the total duration of the dynamic run or particular time intervals within the whole trajectory.

In fact, let us consider dynamics of an N -particle system in a potential force field in a three-dimensional space. Let m_1, m_2, \dots, m_N denote the masses of particles, $q_1(t), q_2(t), \dots, q_{3N}(t)$ being their Cartesian coordinates and $p_1(t), p_2(t), \dots, p_{3N}(t)$ their momenta components. Here, the first three $q_1(t), q_2(t), q_3(t)$ position coordinates and the corresponding $p_1(t), p_2(t), p_3(t)$ momenta are those of the first

particle; $q_4(t), q_5(t), q_6(t)$ and $p_4(t), p_5(t), p_6(t)$ are those of the second particle; and so on. At any fixed $t \in [0, T]$ time interval, the $(q_1(t), q_2(t), \dots, q_{3N}(t), p_1(t), p_2(t), \dots, p_{3N}(t))$ vector specifies a $(\vec{q}(t), \vec{p}(t))$ element of a $6N$ -dimensional $R^{3N} \times R^{3N}$ phase space, where $\vec{q}(t) \in R^{3N}$, $\vec{p}(t) \in R^{3N}$.

The problem consists in decomposing a trajectory as $\vec{q}(t) \in R^{3N}$ or $\vec{p}(t) \in R^{3N}$ into orthogonal components (modes) in the corresponding R^{3N} subspace so that the modes are ordered according to the decrease in their time-averaged fractions of the total kinetic energy. In order to reduce the problem of determining the effective modes to the estimation of principal components, it is reasonable to consider the mass-weighted $\vec{p}(t) \in R^{3N}$ trajectory:

$$\left(\frac{p_1}{\sqrt{2m_1}}, \frac{p_2}{\sqrt{2m_1}}, \frac{p_3}{\sqrt{2m_1}}, \frac{p_4}{\sqrt{2m_2}}, \frac{p_5}{\sqrt{2m_2}}, \frac{p_6}{\sqrt{2m_2}}, \dots, \frac{p_{3N-2}}{\sqrt{2m_N}}, \frac{p_{3N-1}}{\sqrt{2m_N}}, \frac{p_{3N}}{\sqrt{2m_N}} \right). \quad (5)$$

Then, the squared norm of the vector at any $t \in [0, T]$ is the instantaneous kinetic energy of the system, while the time-averaged kinetic energy can be obtained by integrating this squared norm divided by the total T duration. To be able to apply the above formulas, one should simply replace

the $\vec{x}(t)$ trajectory in Eqs. (1) and (2) with the one defined by Eq. (5).

In practice, vector (5) can be obtained by multiplying the $\vec{p}(t)$ vector by a diagonal matrix with the following diagonal elements:

$$\left(\frac{1}{\sqrt{2m_1}}, \frac{1}{\sqrt{2m_1}}, \frac{1}{\sqrt{2m_1}}, \frac{1}{\sqrt{2m_2}}, \frac{1}{\sqrt{2m_2}}, \frac{1}{\sqrt{2m_2}}, \dots, \frac{1}{\sqrt{2m_N}}, \frac{1}{\sqrt{2m_N}}, \frac{1}{\sqrt{2m_N}} \right).$$

If the latter matrix is denoted as $\hat{E}^{1/2}$, then vector (5) can be written as $\hat{E}^{1/2}\vec{p}(t)$. And, as was already mentioned, the squared norm of the $\hat{E}^{1/2}\vec{p}(t)$ vector equals the kinetic energy of the N -particle system: $E = \|\hat{E}^{1/2}\vec{p}(t)\|^2$, $t \in [0, T]$. To determine the orthonormal basis in R^{3N} , which represents the effective modes, let us decompose $\hat{E}^{1/2}\vec{p}(t)$, $t \in [0, T]$, into $(\hat{E}^{1/2}\vec{p}(t), \vec{g}_i)\vec{g}_i$ components ($\vec{g}_i \in R^{3N}$, $i = 1, \dots, 3N$) with the following properties.

(1) The m th partial sum

$$\sum_{i=1}^m (\hat{E}^{1/2}\vec{p}(t), \vec{g}_i)\vec{g}_i \quad (6)$$

determines the part of the $\hat{E}^{1/2}\vec{p}(t)$ vector function, for which $\frac{1}{T} \int_0^T \|\sum_{i=1}^m (\hat{E}^{1/2}\vec{p}(t), \vec{g}_i)\vec{g}_i\|^2 dt$ is the time-averaged kinetic energy of the system that is maximum among all $\sum_{i=1}^m (\hat{E}^{1/2}\vec{p}(t), \vec{g}'_i)\vec{g}'_i$ m th partial sums estimated for any orthonormal basis sets $\{\vec{g}'_i\} \in R^{3N}$.

(2) The m th partial sum (6) approximates the time-averaged kinetic energy of the system with the highest accuracy among all the m th partial sums.

As follows from the above discussion, the desirable $\{\vec{g}_i\} \in R^{3N}$ orthonormal basis set, which determines the effective modes of the kinetic-energy decomposition, is the basis composed of the eigenvectors of a linear operator $G: R^{3N} \rightarrow R^{3N}$, the action of which on any $\vec{z} \in R^{3N}$ vector is defined as

follows:

$$\begin{aligned} G\vec{z} &= \frac{1}{T} \int_0^T \hat{E}^{1/2}\vec{p}(t)(\hat{E}^{1/2}\vec{p}(t), \vec{z})dt \\ &= \frac{1}{T} \int_0^T \hat{E}\vec{p}(t)(\vec{p}(t), \vec{z})dt, \end{aligned} \quad (7)$$

where $\hat{E}: R^{3N} \rightarrow R^{3N}$ is a linear Hermitian operator, whose matrix is diagonal in the natural basis of the R^{3N} space: $\hat{E}_c = \text{diag}\{1/(2m_1), 1/(2m_1), 1/(2m_1), \dots, 1/(2m_N)\}$. Basis vectors $\{\vec{g}_i\} \in R^{3N}$ should be ordered in such a way that $\lambda_1^2, \lambda_2^2, \dots, \lambda_{3N}^2$ eigenvalues, which correspond to $\vec{g}_1, \vec{g}_2, \dots, \vec{g}_{3N}$ eigenvectors, fit in the inequality series: $\lambda_1^2 \geq \lambda_2^2 \geq \dots \geq \lambda_{3N}^2 \geq 0$. Thus, the system dynamics can be treated as a superposition of $(\vec{q}(t), \vec{g}_i)\vec{g}_i$ effective modes with the following properties.

(1) They meet the aforementioned extreme requirements.

(2) The time-averaged kinetic energy of a particular $(\vec{q}(t), \vec{g}_i)\vec{g}_i$ effective mode ($i = 1, \dots, 3N$) equals $\frac{1}{T} \int_0^T (\hat{E}^{1/2}\vec{p}(t), \vec{g}_i)^2 dt = \lambda_i^2$.

(3) The fraction of the time-averaged kinetic energy accumulated on m effective modes $(\vec{q}(t), \vec{g}_i)\vec{g}_i$ equals $\vartheta_m = (\sum_{i=1}^m \lambda_i^2) / (\sum_{i=1}^{3N} \lambda_i^2)$.

To finish the discussion, let us add three comments.

Comment 1. The method can be used for constructing effective modes that enable one to decompose the system dynamics in the extreme approximation for any time-averaged $Q(t)$ dynamic parameter of the $\vec{x}(t) \in R^n$ trajectory, which can

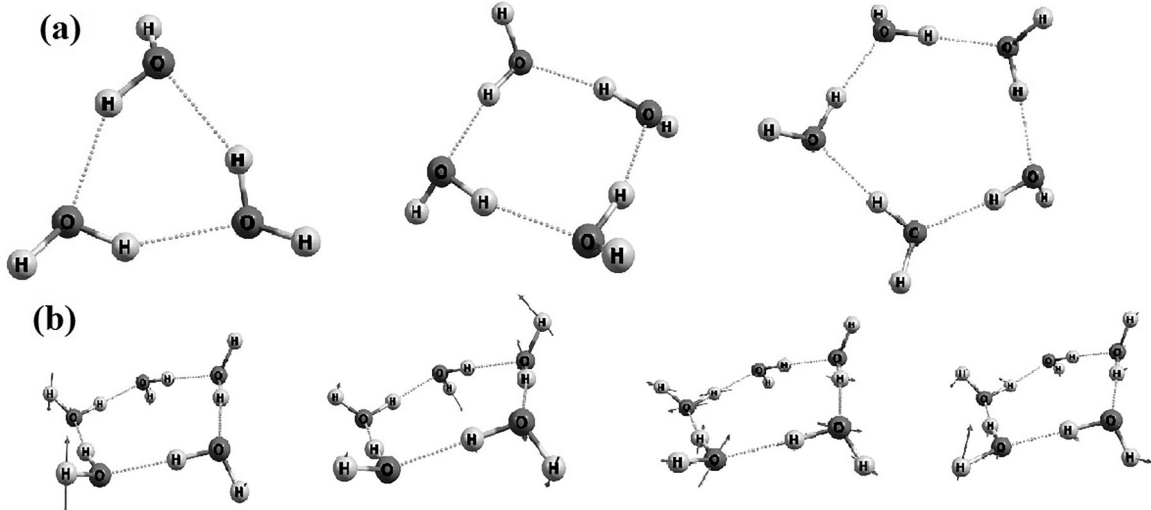


FIG. 1. (a) The optimum structures of a water trimer, tetramer, and pentamer and (b) the shapes of active normal-mode vibrations (from left to right): twisting, pleating, canting, and breathing combined with rocking.

be estimated at any time moment based on the phase trajectory data as follows: $Q(t) = \|\hat{Q}^{1/2}\bar{x}(t)\|^2 = (\bar{x}(t), \hat{Q}\bar{x}(t))$, where $\hat{Q} = (\hat{Q}^{1/2})^* \hat{Q}^{1/2} : R^n \rightarrow R^n$, the star denotes the conjugation, and $\hat{Q}^{1/2} : R^n \rightarrow R^n$ is a linear operator.

Comment 2. The above variant $\hat{E}^{1/2}\bar{p}(t)$ is especially reasonable for the analysis of the character of the governing effective modes within diverse time intervals as related to the coupling of normal modes and the energy redistribution among them in the system of interest due to the same mass-weighted definition of the coordinates.

Comment 3. If the phase trajectory is defined as a set of values at discrete time moments $t_k = (k-1)\Delta$, $k = 1, 2, \dots, K$, then matrix elements of the X linear operator defined according to Eq. (2) are $X_{ij} = \frac{1}{K} \sum_{k=1}^K x_i(t_k)x_j(t_k)$, $i, j = 1, \dots, n$, while the elements of the G linear operator defined by Eq. (7) are $G_{ij} = \frac{1}{K} \sum_{k=1}^K \frac{p_i(t_k)p_j(t_k)}{2\sqrt{m_i^{(i-1)/3+1}m_j^{(j-1)/3+1}}}$, $i, j = 1, \dots, 3N$, where $[z]$ is the floor function of z . Subscripts in the denominator are selected in such a way that $p_{3s-2}, p_{3s-1}, p_{3s}$ momentum components of the s th particle are divided by $\sqrt{2m_s}$, $s = 1, \dots, N$.

In this paper, the effective modes that provide the most accurate approximation of the kinetic energy of a cluster are considered. The N_{eff} number of the effective modes is estimated as follows:

$$N_{\text{eff}} = \exp\left(-\sum_{j=1}^N \theta_j \cdot \ln(\theta_j)\right). \quad (8)$$

Here, $\theta_j = \frac{\langle E_j[\bar{p}(t)] \rangle}{E}$ is the kinetic-energy fraction ($\langle E_j[\bar{p}(t)] \rangle$) accumulated in the j th mode normalized to the E kinetic energy of the cluster averaged over the whole trajectory.

III. MODEL SYSTEMS AND TRAJECTORY GENERATION

As was mentioned above, water clusters are interesting subjects for the effective-mode analysis, because they are stabilized by hydrogen bonds, which, on one hand, are

intermolecular interactions of weak or moderate strength and substantial anharmonicity and, on the other hand, provide collective effects that inevitably should be manifested in the peculiarities of cluster dynamics. To test the method proposed and demonstrate its possibilities in drawing meaningful conclusions about the character of collective dynamics, small $(\text{H}_2\text{O})_n$ clusters composed of three to five water molecules were selected (Fig. 1). The dynamic trajectories were generated in Born-Oppenheimer molecular dynamic simulations. Despite the large number of various-level semiempirical potentials up to the advanced variants including polarizable Thole type model and atomic multipole optimized energetics for biomolecular applications variants and explicit many-body polarizable potential families [38], we opted for the nonempirical potential, which can be estimated as a solution of the electronic Schrödinger equation and implies the absence of any predefined force field components. The reason for that lies in the possibility of unrestricted variations in the mutual arrangement of the nuclei up to the dissociation of the system into particular components accompanied by the corresponding electron density redistribution, which is impossible in terms of any parametrized model. For solving the equation, the second order of the Møller-Plesset perturbation theory was used. The method was repeatedly proved to be adequate for the description of hydrogen-bonded systems that involve the first- and second-row elements of the periodic table. The basis set used was of the triple-zeta quality, namely, 6-311G augmented with diffuse and polarization functions on all nuclei [6-311++G(d, p)], which is sufficiently flexible to provide a reliable description of the electron density redistribution upon the formation, distortion, or breakage of hydrogen bonds and, at the same time, sufficiently compact to eliminate the linear dependence of basis functions.

The dynamic trajectories were generated as follows. At first, optimum configurations of the clusters were found [Fig. 1(a)], and their correspondence to the true minima was proved by the normal-coordinate analysis. Thus, at the starting point, information about the normal modes of the clusters was available. Different variants of the initial conditions of

TABLE I. Model water clusters and their initial excitation energies (E_{exc} , kcal/mol).

(H ₂ O) ₃	E_{exc}	3.6	7.2	10.7	14.3
	Notation	W3_1	W3_2	W3_3	W3_4
(H ₂ O) ₄	E_{exc}	6.2	12.3	18.5	24.6
	Notation	W4_1	W4_2	W4_3	W4_4
(H ₂ O) ₅	E_{exc}	7.6	15.2	22.7	30.3
	Notation	W5_1	W5_2	W5_3	W5_4

the dynamic propagation were considered, but all of them mimic an excitation that is possible under particular thermal conditions, which was provided by the excitation of those normal modes solely whose frequencies fall below 210 cm^{-1} . The modes in this spectral range are all strongly delocalized and represent diverse distortions of the model cluster rings, namely, breathing (extension and contraction), canting, twisting, pleating, and rocking of molecules [schematically shown in Fig. 1(b)]. A small portion of the translational motion was also supplied to the cluster at the accurately zero rotational momentum. Such excitation predetermines the initially nearly uniform excess energy distribution over the whole cluster, so that any drastic reorganization of the cluster can only be a consequence of a substantial energy redistribution, particularly its accumulation on a few degrees of freedom, which makes it possible to retrieve information about the coupling of diverse modes and the corresponding energy flows. Series of excitations of a regularly increasing energy were considered for each cluster. The excitation energies involved in the analysis and the corresponding notations of dynamic trajectories are listed in Table I.

Several aspects should be noted. First of all, the number of normal vibrations that obey the above criterion increases with an increase in the number of water molecules involved in the cluster and equals 6 in a trimer, 10 in a tetramer, and 14 in a pentamer. Therefore, even the lowest initial excitation energy normalized to the number of molecules increases from 1.2 kcal/mol in a trimer to ≈ 1.5 kcal/mol in a tetramer and a pentamer. Next, an average H-bond energy, which was estimated as the total dissociation energy of the cluster into individual water molecules divided by the n number of bonds (or, equally, the number of molecules) also changes with the cluster size, being equal to 5.0, 6.5, and 6.8 kcal/mol at $n = 3, 4,$ and 5 . As one can see, already Wn_2 trajectories formally meet the conditions when the total energy accumulated by the cluster is sufficient for the breakage of at least one hydrogen bond. The latter process requires the localization of energy on particular vibrational degrees of freedom, but the initial excitation energy, as was already stressed above, was always quite uniformly distributed over all the molecules involved, which made the dissociation unlikely at least within the initial period of dynamic propagation. At the same time, the highest excitation energy in the case of all the clusters considered is already sufficient for the decomposition of the clusters with the formation of more or less independent fragments. Thus, the conditions involved in the consideration enable one to judge not only the character of the excess energy redistribu-

tion within the cluster and, hence, the character of the most meaningful effective modes, but also the possibility of the excess energy localization on particular degrees of freedom that may lead to the dissociation. The conclusions drawn below are based on the results of the dynamic propagation of water clusters at the aforementioned initial conditions with the whole lengths of trajectories of 50 to 100 ps at time steps of 0.5 fs, which was found to be the largest possible value that provided the energy conservation even at the highest activation energy considered. At the same time, it is quite small, providing not as substantial shifts in the positions of all the nuclei. The smaller values may be necessary only for constructing reliable dipole moment or polarizability dependences on the effective structure coordinates, but insofar as the investigation was not aimed at constructing absorption or scattering spectra of the systems, the smaller steps were not required.

IV. DYNAMIC EFFECTS IN SMALL WATER CLUSTERS IN TERMS OF THE EFFECTIVE-MODE ANALYSIS

First of all, it is expedient to analyze the activation of modes for all the clusters depending on their initial excitation energy. This characteristic can be deduced from the distribution of the trajectory-averaged kinetic energy of the cluster over the effective modes. For a water trimer, the effect is illustrated by Fig. 2. The numbers of effective modes depending on the mean kinetic energy were estimated according to Eq. (8). It is worth noting that the total number of the degrees of freedom of the trimer equals 27, but three of them correspond to the rotational motion, which is not activated in the dynamic runs under consideration. Therefore, the maximum possible number of active degrees of freedom, including the translational motion, is 24. As follows from Fig. 2(b), it is nearly reached at the highest excitation energy considered. At the same time, when the energy is by half and by a third smaller, the number of effective modes is nearly the same, which is in full agreement with the character of the kinetic-energy distributions [Fig. 2(a)]. Furthermore, with an increase in the overall excitation of the cluster, the distribution gradually approaches the one when the trajectory-averaged energy accumulated on each of the largest number of modes, namely, 18 (which is only by three smaller than the number of the vibrational degrees of freedom), is nearly the same, an average of $\approx 4.1\%$ (falling in a range of 3.7 to 4.5%). Accordingly, the potential-energy increments of the cluster again averaged over the 50-ps trajectories ($\langle \Delta E_{\text{pot}} \rangle$) increase from ≈ 1.9 to 9.3 kcal/mol (Table II) with an increase in the excitation energy (Table I). Naturally, these are mean values, and the actual potential-energy oscillations around them are quite large. These oscillations reflect how substantial the structure changes can be due to the temporary localization of the kinetic energy on particular degrees of freedom, and this aspect is touched upon in detail below, while the averaged values characterize the mean distortion level of the cluster. This level naturally increases with an increase in the initial excitation, but, as follows from the data of Table II, it is not proportional to the latter. It increases from an average of 55% for trajectories W3_1, W3_2, and W3_3 to 65% for W3_4, which means that the highest excitation corresponds to the strongest time-averaged distortion of the cluster, which,

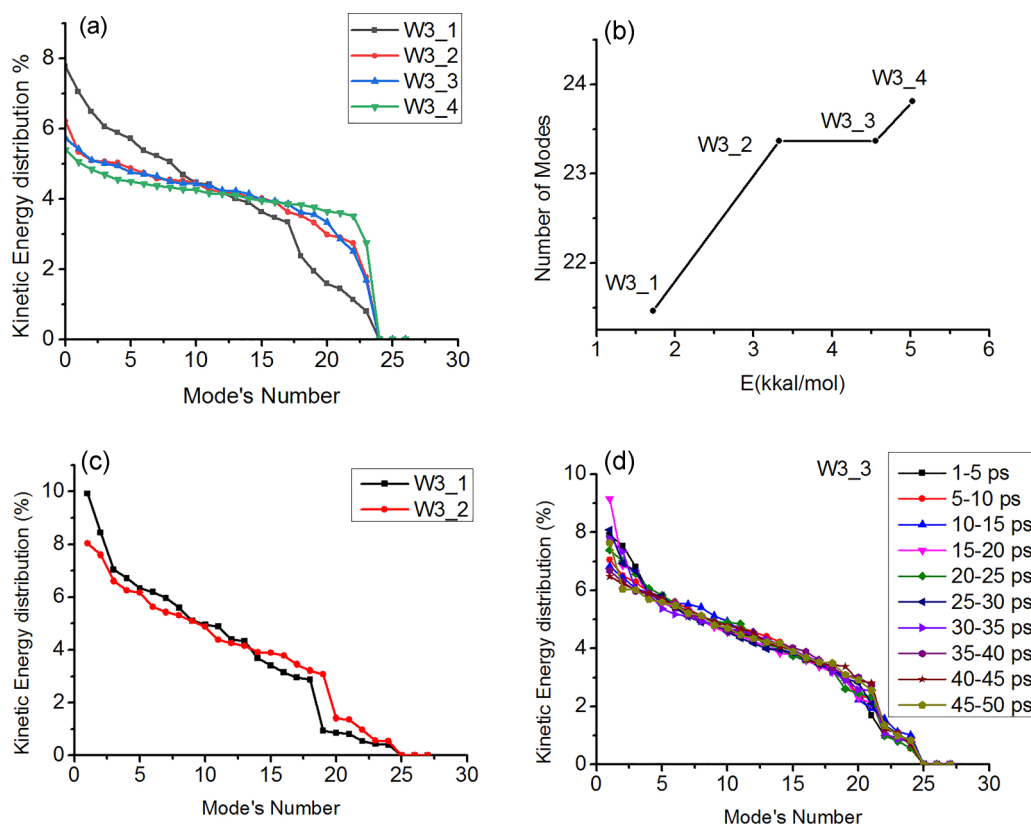


FIG. 2. (a) The effective-mode distribution of the kinetic energy of a water trimer averaged over the whole trajectory at different initial conditions (see Table I), (b) the corresponding number of effective modes, and (c), (d) the effective-mode distribution of the mean kinetic energy within 5-ps intervals (c) for W3_1 and W3_2 trajectories within the first 5 ps of propagation and (d) for the W3_3 trajectory within all 5-ps intervals.

hence, has a lower additional kinetic energy (normalized to the number of degrees of freedom) at its disposal.

What happens to the trimer structure at the above excitations? This is clearly illustrated by the shapes of effective motions (represented by the corresponding eigenvectors g_i ; see above) that prevail within different time intervals. When the smallest activation energy (≈ 3.6 kcal/mol) is supplied to the cluster [Fig. 2(c)], the highest eigenvalues correspond to breathing, swinging, canting, and two rocking motions coupled to swinging. Judging from the overlap integrals of the effective and normal-mode vectors, each effective mode can be considered as a superposition of the basic normal motions. Moreover, it is impossible to distinguish the leading contributions of particular normal modes, because typically the largest amplitudes fall in a range of 0.15 to 0.70, so that 6

TABLE II. Trajectory-averaged potential-energy increments ($\langle \Delta E_{\text{pot}} \rangle$, kcal/mol) of the model clusters.

	Trajectory	W3_1	W3_2	W3_3	W3_4
(H ₂ O) ₃	$\langle \Delta E_{\text{pot}} \rangle$	1.9	3.9	6.1	9.3
(H ₂ O) ₄	Trajectory	W4_1	W4_2	W4_3	W4_4
	$\langle \Delta E_{\text{pot}} \rangle$	3.4	6.9	11.14	16.2
(H ₂ O) ₅	Trajectory	W5_1	W5_2	W5_3	W5_4
	$\langle \Delta E_{\text{pot}} \rangle$	4.0	8.3	13.1	18.5

to 12 coupled oscillators determine each effective distortion character. As a result, these coupled motions predetermine the general structure transformations. The governing effective modes themselves change their roles, which is manifested in the structure of the overlap matrices of the modes that characterize the dynamic changes in the cluster within successive 2-ps-long intervals. At this lowest excitation of the trimer, the top left 9×9 block of the matrices can distinctly be distinguished (the corresponding elements are at least an order larger than the residual ones in the same rows and columns of the matrix) within the first 10 ps of the dynamic propagation, which means that the governing motions preserve their character, but a certain energy redistribution between the modes takes place. Accordingly, OH_f fragments (where the f subscript denotes a “free” hydrogen atom uninvolved in hydrogen bonds) of the molecules are flipping from time to time, typically in pairs or sequentially, so that the one initially located above the oxygen plane becomes oriented downwards, while an adjacent one changes its location in an opposite way. As a result, all three H_f atoms can be found sometimes at the same side of the oxygen plane, which is untypical of an energetically favorable arrangement. Swinging motions distort hydrogen bonds between the molecules from time to time, but the latter are always quite rapidly restored, and the amplitude of the motions is insufficient for such a reorientation of the molecules that may provide the inversion of the H-bond sequence from clockwise to counterclockwise.

The corresponding changes proceed in a kind of waves over the cyclic trimer.

Generally similar trends can be noticed in the dynamics of the trimer at twice as large excitation (W3_2 trajectory), which corresponds to twice as high mean kinetic energy localized on the effective modes and nearly twice as large potential-energy increment. Hence, the amplitudes of breathing, canting, and swinging motions mixed with rocking in the latter case [which correspond to five highest eigenvalues, Fig. 2(c)] are noticeably larger. Additionally rocking combined with wagging (two next eigenvalues) begins to play a substantial role. All these effective motions provide such an amplitude of OH oscillations that the protons involved and uninvolved in a hydrogen bond can swap around, though the direction of bonding remains the same. The latter is predetermined by the fact that the excitation energy is sufficient for the swapping within only one molecule at a time.

When the additional total energy is still nearly by half higher (W3_3) but distributed at a close mean potential-energy-increment to kinetic-energy-increment ratio, the same kinds of motions correspond to the eigenvalues that fall in a still narrower range [Fig. 2(d), 1–5-ps interval], which reflects their nearly concurrent activation. This variant of the excess energy distribution provides much quicker swapping and half rotation of molecules so that hydrogen bonds between them are noticeably weakened, and already by 2.5 ps one of them is broken, and the whole cluster transforms into a bended chain. However, the chain survives for no more than 0.5 ps, and the closed trimolecular ring is restored. Later on, such more or less complete folding and unfolding of the chain into the ring and backwards takes place in ≈ 1 ps. No other principal changes can be noticed in the dynamics of the cluster compared to the W3_2 trajectory, and this fact correlates quite well with nearly the same character of the kinetic-energy distribution in the effective modes for these two situations [Fig. 2(a)] and is reflected in apparently the same number of the effective modes that do determine the character of motions [see Figs. 2(c) and 2(d)], but a slightly higher mean kinetic energy provides conditions for more noticeable distortions [Fig. 2(b)].

If we now analyze the time dependence of the kinetic-energy distributions within successive 5-ps intervals [Fig. 2(d)], an interesting peculiarity can be noticed. The resulting mean energy distribution characterized by an extended plateau [Fig. 2(a)] gradually arises from the steeper descending curves, each of which has much in common with the mean energy distribution in the case of W3_1 trajectories or with the distribution for the initial 5-ps time interval [Fig. 2(c)]. However, the leading effective modes (that correspond to the highest eigenvalues) are replacing each other with time. For example, the leading breathing modes activated from the very beginning of the dynamic evolution (in the first 5 ps) fully restore their role only by 45 ps. In between, the alternating key modes are of the swinging (5–10 and 20–25 ps) and distortion (10–20 and 25–30 ps) kinds, which concurrently contribute to the dynamics in a 30–40-ps interval. As a result, the excess energy transfer between different sets of effective modes upon integration over the whole time interval produces a picture of a nearly uniform mean energy distribution in diverse effective modes.

Further increase in the excitation energy (W3_4 trajectory) adds to the possibilities of the molecules in their concurrent but nearly independent (due to the increased intermolecular distances) large-amplitude oscillations, which can result in local reorientations of molecules and the concurrent inversion of the H-bond directions between them. Such a reorganization in combination with the weakening of the residual bonds enables the transformation of the ringlike structure into an open chain, which having passed through a straight-line configuration can bend the other way, which corresponds to the formal reordering of molecules within the ring. With time, a similar transformation cycle becomes possible for any molecule as central in the transient chainlike configuration, which results in all possible permutations of molecules in the closed structure. When not only one but simultaneously two hydrogen bonds are weakened, the trimer apparently dissociates into a more or less distorted dimer and a monomer, and such a repeated process becomes prevailing after 10 ps of the dynamic evolution. The corresponding averaged (over 2- to 3-ps intervals) configurations of the cluster can be represented by not as substantially bent trimolecular chains or combinations of a dimer and a monomer at different mutual orientations. These transformations (partial breakage of intermolecular bonds leading to the visible permutations of molecules) are possible due to the increased mean potential-energy-increment to kinetic-energy-increment ratio (65% compared to the above values of 53 to 57%). The corresponding additional degree of freedom is clearly reflected by the increased number of effective modes of the cluster [Fig. 2(b)] at the more uniform energy distribution in the larger number of modes [Fig. 2(a)].

In the case of the tetramer, the activation of modes and their involvement in the 50-ps dynamics are illustrated by Fig. 3. It is worth noting that here the mean potential-energy to kinetic-energy ratios (Table II) are higher than those typical of the trimer, namely, as the excitation energy increases, the mean potential-energy increment increases from 55 and 56% in the case of W4_1 and W4_2 trajectories to 60 and 66% in the case of W4_3 and W4_4 trajectories. Therefore, though the observed trends are generally similar to those distinguished in the case of the trimer, there are certain differences. First of all, there is no such scattering of the mean kinetic energy even at the lowest excitation energy. Next, the system with the highest excitation energy (W4_4 trajectory) is characterized by a very pronounced plateau of the distribution function, which corresponds to as much as 27 degrees of freedom (similar to that in the trimer taking into account the total numbers of the degrees of freedom of these clusters), the contributions of each of which to the total mean kinetic energy fall in a very narrow range of 2.6 to 3.3%, being equal on the average to 2.9%. The largest possible number of translational and vibrational degrees of freedom is activated at the highest excitation energy of the cluster, which shows again that the conditions selected are sufficiently broad to deduce valuable information about the cluster dynamics. And these dynamics changes with an increase in the activation energy are as follows.

At the lowest excitation energy (W4_1 trajectory), which is ≈ 1.55 kcal/mol per molecule (compared to 1.2 kcal/mol for the trimer in the W3_1 run), the structure changes are driven from the very beginning by the following effective modes [in the decreasing order of the corresponding eigenvalues,

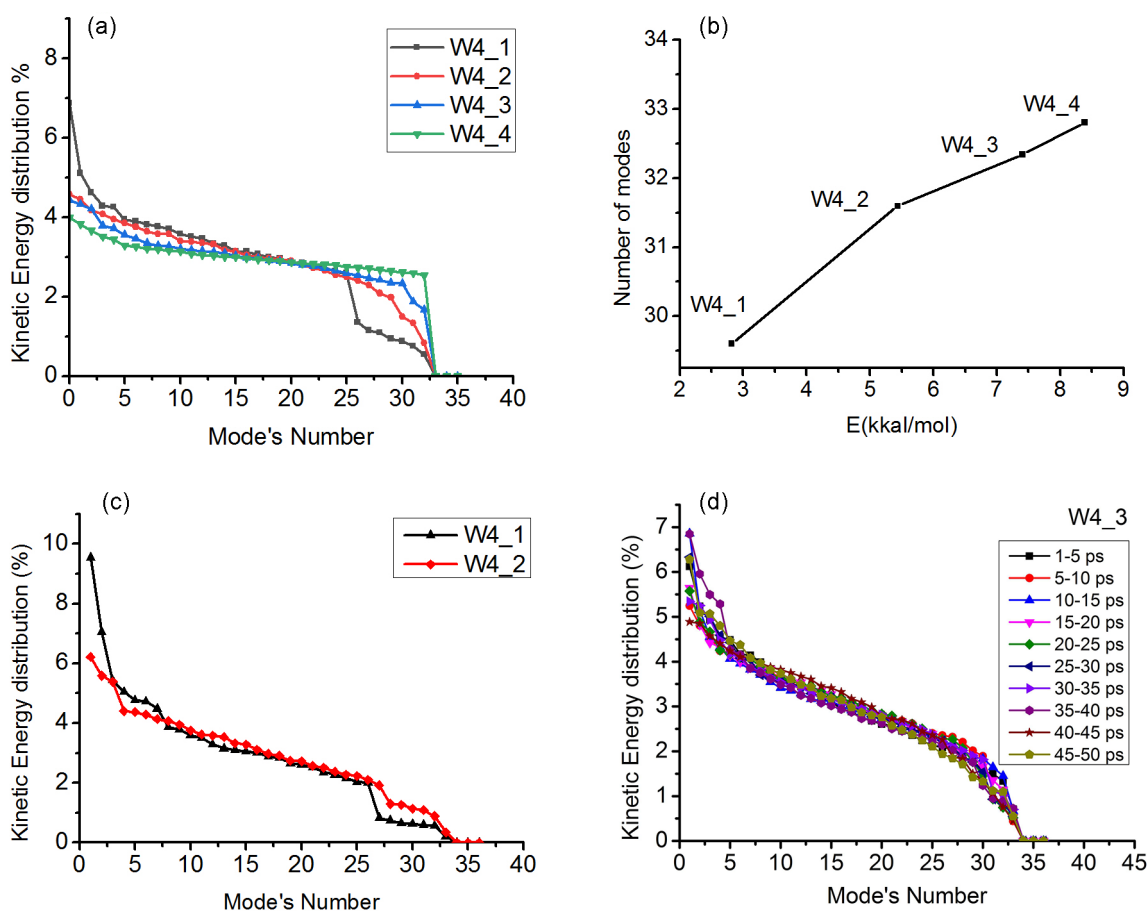


FIG. 3. (a) The effective-mode distribution of the kinetic energy of a water tetramer averaged over the whole trajectory at different initial conditions (see Table I), (b) the corresponding number of effective modes, and (c), (d) the effective-mode distribution of the mean kinetic energy within 5-ps intervals (c) for W4_1 and W4_2 trajectories within the first 5 ps of propagation and (d) for the W4_3 trajectory within all 5-ps intervals.

Fig. 3(c)]: breathing, pleating (along the spatial diagonal of the ring), and canting of rhombic and trapezoid characters of the ring, as well as two swinging and two rocking motions of the molecules. The larger amplitudes of the oscillations correlate well with the larger mean potential-energy increment ($\approx 55\%$); however, the total excitation energy is insufficient for drastic changes within the bonded cluster. Upon the twice as large activation of the cluster that corresponds to the mean activation energy per molecule of ≈ 3.1 kcal/mol, which is intermediate between those typical of W3_2 and W3_3 trimer dynamic runs, a slightly different ranking of the effective modes in the first 5 ps of the dynamic propagation can be noticed. The contributions of pleating and breathing distortions of the molecular ring become nearly equal at a level typical of canting in the lower-energy dynamics [Fig. 3(c)], pleating being the leading among them. The next effective modes are combinations of swinging, rocking, and breathing motions with varying weights. Here, changes in the character of the governing effective modes deserve mention. The structure of the overlap matrix of the effective-mode vectors within successive 2-ps intervals changes as follows. Up to 6–8 ps, the whole matrix and even its top left corner block are noticeably sparse (the largest nondiagonal elements are 0.4 to 0.8 compared to the diagonals that vary from 0.02 to

0.4). Within the subsequent 6 ps, the overlap matrix becomes gradually less sparse, and by 20 ps its top left 8×8 block is nearly tridiagonal (in a sense that the corresponding elements are ≈ 0.5 – 0.8 and, thus, at least half an order larger than the residual ones). Then, a second round of energy redistribution takes place, which ends by 24–26 ps, which is again manifested in the nearly tridiagonal 8×8 block. And so on. As a result, the temporary breakage of some hydrogen bonds becomes possible due to either the breathing of the ring or the swinging of molecules at certain time intervals predetermined by particular kinetic-energy transfer within the cluster. Here, the flipping of molecules typical of the trimer in its W3_2 trajectory is already accompanied by swapping noticed in the case of W3_3 evolution, which shows that such changes become possible when the excitation energy, which is formally lower when normalized to the number of molecules, can be redistributed within the cluster and accumulated on the proper degrees of freedom of a particular particle. Note that the mean potential-energy increment per molecule in the case of the W4_2 trajectory is 1.7 kcal/mol compared to 1.3 and 2.0 in the case of W3_2 and W3_3 sets of trajectories for the trimer. Such a redistribution takes place due to the correlation in the states (particularly, vibrational states) of the molecules bound via hydrogen bonds to each other. Naturally, in the absence

of such interactions, the necessary consistent flowing of the kinetic energy would be impossible.

The next set of trajectories (W4_3) corresponds to still higher activation energy, ≈ 4.6 kcal/mol per molecule, which is already close to the normalized activation energy supplied to the trimer at its highest excitation (4.8 kcal/mol). However, here the mean potential-energy increment is lower, ≈ 60 vs 65% in the trimer. Therefore, quite expectedly, local distortions of the tetramer are driven by temporary breakages of hydrogen bonds and the respective reorganization in the mutual arrangement of molecules. According to the temporarily prevailing mean configuration of the cluster, the weights of some effective modes increase, while those of some others decrease. For example, the reciprocal shifts of molecules that dominate in the first 5-ps interval give the pass to pleating within 5–10- and 10–15-ps intervals, the prevalence being sometimes quite substantial [see curves in Fig. 3(d)]. Here, it is worth noting that in the trimer the breakage of a hydrogen bond results in the opening of the trimolecular ring and the decrease in the total number of intermolecular contacts by 1. In the tetramer, the breakage of one hydrogen bond within a ring is typically accompanied by the closing of a trimolecular cycle, the fourth molecule being kept attached to a vertex of the triangle via the already existing unbroken bond. The unchanged number of hydrogen bonds predetermines the aforementioned smaller potential-energy increments, which nevertheless enable not only flipping, but also swapping of OH bonds in individual molecules. At the same time, the mutual arrangement of the triangle and the fourth molecule may be any between the nearly coplanar and pyramidal ones, the latter being a transient between the two closed tetramolecular ring configurations, which differ by a transposition of the two neighboring molecules of the ring. This transformation can be described quite reasonably already with a sole effective mode, namely, the aforementioned pleating of the tetramolecular ring along its diagonal. Taking into account that the mean frequency of this effective mode is close to 30 cm^{-1} , its excitation can be estimated as nearly sixfold, which is actually sufficiently high to promote the transformation of a nearly planar quadrangle into a pyramid. Later on, the leading role is transferred to effective modes that correspond chiefly to moderate-amplitude breathing of the cluster with frequencies about four times as high as that of the pleating motion.

Thus, the larger the number of intermolecular contacts between molecules, the broader the possibilities for the rearrangement of the latter at nearly the same mean excitation energy per molecule and the close potential-energy-increment to kinetic-energy-increment ratio. However, a drastic reorganization can take place only when a sufficient kinetic energy is localized on proper degrees of freedom, which becomes a progressively rarer event with an increase in time when the mean energy distribution becomes more uniform, and the leading effective modes are more strongly delocalized [see Figs. 3(c) and 3(d)]. Nevertheless, the possible formation of different structures stabilized by the same number of hydrogen bonds promotes permutations of molecules in the tetramer at an activation energy per molecule lower than that found necessary in the case of the trimer (≈ 4.6 vs 4.8 kcal/mol).

At still higher activation energy (W4_4 trajectories), all the transformations described above become possible already

within the first 1.5 ps of the dynamics. Moreover, the resulting transpositions of molecules are accompanied by the inversion of the hydrogen-bond sequence from clockwise to counterclockwise, and transient configurations may be either chainlike or pyramidal, or elongated rhombic with an interlink (which makes the structure resemble two fused triangles), or a triangle with a side molecule. Such changes result from various gradually interchanging combinations of effective motions (wagging, swinging, and winging of all molecules) with nearly the same mean kinetic energies: as one can judge based on Fig. 3(a), this dynamic evolution is characterized by the most uniform kinetic-energy distribution over the largest number of effective modes. It is worth noting that the structure averaged over the first 5 ps of the dynamics resembles a combination of two dimers, which shows that there are certain correlations in the states of the closest molecules in the system despite their visible noticeable reciprocal shifts. Later on, the effective averaged configurations resemble, for example, a tetramolecular zigzag chain in 5–10- and 15–20-ps intervals or a trimer with a side molecule in a 10–15-ps interval that is replaced with two dimers in a 20–25-ps interval. In fact, though the structures are visually different, the aforementioned correlation between the adjacent molecules in pairs is always preserved.

If one turns to the pentamer, both certain similarities and differences can be noticed. Although the initial activation energies per molecule are close to the values of the tetramer (Table I), the mean potential-energy increment differs (Table II): it is an average of $\approx 54\%$ for W5_1 and W5_2 trajectories and an average of $\approx 59\%$ for W5_3 and W5_4 ones. Thus, the first two are similar to those of the low excited trimer, while the two residual ones are smaller than the largest values found in the case of both the trimer and tetramer. As a result, the mean kinetic energy of the cluster is as large as 2.4 kcal/mol per molecule in W5_4 dynamic runs [Fig. 4(b)]. In general, the mean kinetic-energy distribution demonstrates not as regular character as was typical of the smaller clusters [Fig. 4(a)]. It does not approach a plateau shape with an increase in the excitation energy: the trend is broken for the W5_4 trajectory. Here, one can see a half-bell-shaped distribution for the first five or six modes and a descending slope for the next ten modes. This means that the dynamic evolution of the cluster drastically differs from all the residual situations. This conclusion is further supported by the numbers of activated effective modes shown in Fig. 4(b). As one can see, the initial gradual increase in the number of modes, which was typical of the smaller clusters, is broken at the highest excitation energy, and the number falls below 41. This is possible only if the cluster is decomposed into smaller fragments, which do not rotate independently. This idea is further supported by the kinetic energy of the cluster [Figs. 4(c) and 4(d)], which increases after 30 ps in the case of the W5_4 trajectory and remains constant at the lower activation in the W5_3 run, as well as the analysis of the structure transformations along the trajectory.

To be consistent, at the lowest activation energy (W5_1 trajectories), quite an expected overall breathing [that corresponds to the highest eigenvalue, Fig. 5(a)] of the pentamolecular ring is accompanied by moderate-amplitude canting of three complementary shapes and twisting of the ring. Only

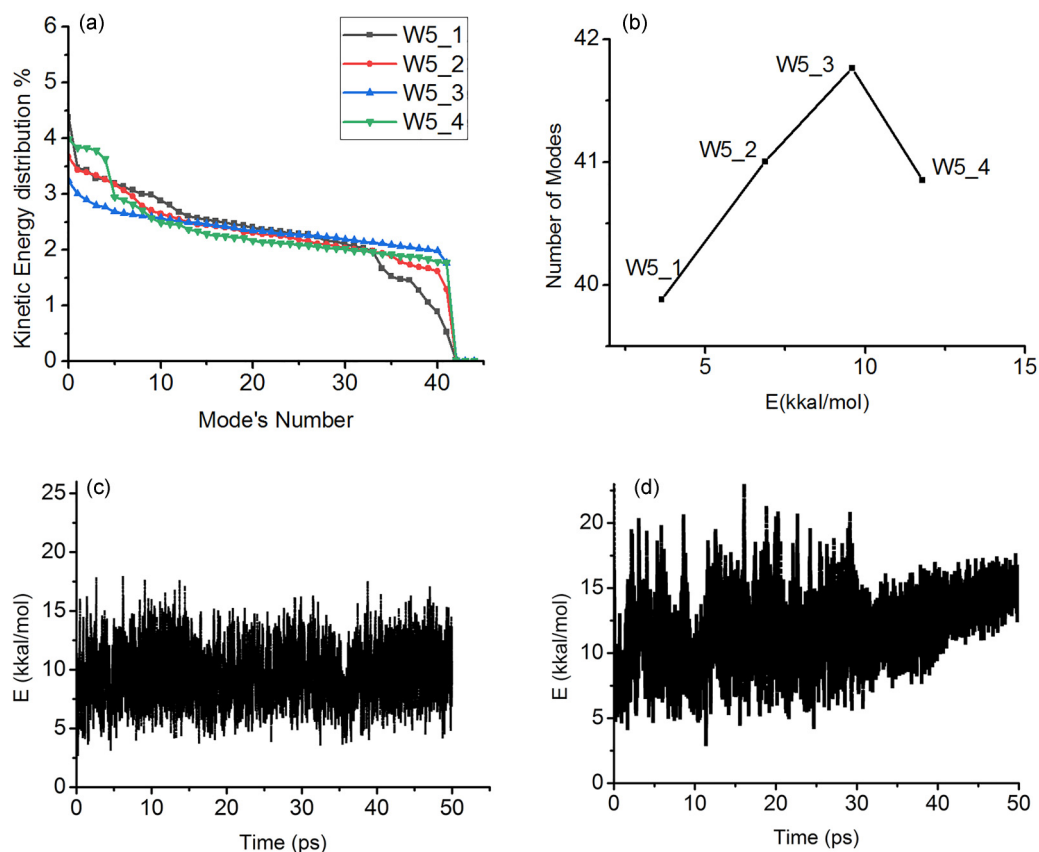


FIG. 4. (a) The effective-mode distribution of the kinetic energy of a water pentamer averaged over the whole trajectory at different initial conditions (see Table I), (b) the corresponding number of effective modes, and (c, d) the kinetic energy of the cluster along the trajectories (c) W5_3 and (d) W5_4.

at this level ($\approx 3.5\%$ contribution to the total kinetic energy) wagging, swinging, and winging motions of molecules appear. Such energy distribution results in flipping of OH_f functional groups from time to time, but nothing special takes place compared to tri- and tetramolecular rings in agreement with a little bit higher mean kinetic-energy fraction at a smaller mean potential-energy increment, which reflects the extent of structure distortions. A twice as large increase in the activation energy (W5_2 trajectories) at the same potential-energy-increment to kinetic-energy-increment ratio (Tables I and II) provides a noticeable wavy motion of the ring: two first canting effective modes are succeeded by three combi-

nations of breathing and twisting distortions, each (the two former and the three latter) contributing a total of ≈ 6 to 7% to the kinetic-energy distribution [Fig. 5(a)]. As a result, in short-term averaged configurations (which resemble an open envelope or a half chair when one molecule does not fall in the plane of the four residuals), a protuberance (the molecule which drops out of the plane) moves along the ring during the dynamic run. Accordingly, hydrogen bonds between the molecules become bifurcated from time to time when both OH groups of one molecule are oriented toward an oxygen nucleus of the neighboring molecule. Such transformations can be viewed as incomplete or half swapping. Full swapping does

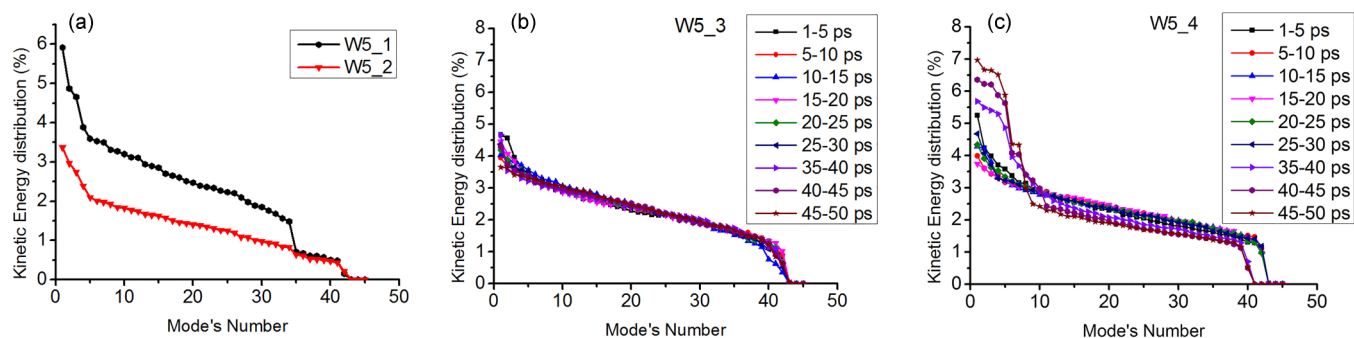


FIG. 5. The effective-mode distribution of the kinetic energy of a water pentamer averaged over 5-ps intervals for (a) W5_1 and W5_2 trajectories in the first 5 ps of propagation and (b, c) W5_3 and (c) W5_4 trajectories within all 5-ps intervals.

not take place despite nearly the same mean dynamic characteristics of penta- and tetramolecular rings. However, this is in agreement with the kinetic-energy distributions in effective modes, which are very close for W5_1 and W5_2 trajectories [Fig. 4(a)] by contrast to smaller molecular rings where the corresponding distributions noticeably differed [Figs. 2(a) and 3(a)]; namely, with an increase in the activation energy, the kinetic energy accumulated on the leading effective modes rapidly decreased to the mean level of the residual ones. Here, the number of modes characterized by the energy percentage above the plateau level reaches nearly 12 for the two sets of trajectories.

A more uniform kinetic-energy distribution is reached upon further increase in the activation energy (W5_3 trajectories) when the aforementioned wavy distortion of the pentamolecular ring transforms into more substantial structure changes. The changes are driven by loosening of intermolecular bonds. If one looks at the energy distribution depending on time within 5-ps intervals along the trajectory [Fig. 5(b)], a previously untypical narrow half-bell-shaped segment in the kinetic-energy distribution within the first 5-ps interval can be noticed, which shows that there are two effective modes that play a key role in the dynamic onset. These modes are breathings with mean frequencies of $\approx 160\text{--}175\text{ cm}^{-1}$ and nearly equal percentages. Later on, the energy distribution curves acquire a typical descending character, the highest percentage being by a quarter smaller in the final 5-ps interval and corresponding to an effective mode of wagging kind with a frequency $\approx 350\text{ cm}^{-1}$. Moreover, within this interval, the mean structure of the cluster is a restored bound pentamolecular ring, and the resulting mean kinetic-energy distribution [Fig. 4(a)] is even closer to a plateau shape than those in the case of W4_4 and W3_4 trajectory sets. This can be treated as another illustration of the collective nature of the effective modes of H-bonded clusters, which provides a rapid redistribution of the excitation energy.

In intermediate time intervals, the envelop flap molecule in the overall ringlike structure may become either nearly coplanar with the residual tetramolecular segment or find itself above it (which resembles a half-closed flap) or migrate toward the opposite edge, thus pushing another molecule and forcing it to acquire the role of a new flap. And all such transformations proceed at the preserved coordination between the molecules. Note that here the mean kinetic-energy increment ($\approx 1.9\text{ kcal/mol}$ per molecule) is close to the largest values observed in the dynamic trajectories of the trimer and tetramer, but the large energy is quite well accumulated by the cluster, which does not undergo any transformation leading to a decrease in the total number of hydrogen bonds: a mean potential-energy increment (Table II) is only 58% compared to 65 and 66% in the trimer and tetramer under comparable conditions.

However, the same collectivity of the dynamic states of the cluster may lead to opposite and quite drastic changes in its structure. As was mentioned above, the collective nature of intermolecular bonds may predetermine the temporary accumulation of large kinetic energy on particular degrees of freedom at certain time moments, and if these degrees correspond to the breakage of some coordinating bonds this will definitely happen. This is the situation we face in the case

of W5_4 trajectories. Here, the activation of the cluster results in the opening of a pentamolecular ring followed by various structure transformations, nearly all of which provide the existence of one molecule coordinated to the residual system via only one hydrogen bond. This system resembles a folded zigzag (up to 10 ps), a twisted or almost flat ringlike tetramer (from 10 to 20 ps), or a trimer with a side molecule when the fifth molecule is attached to either the side one (20–25 ps) or another vertex of a triangle (25–30 ps). Accordingly, the character of the first (leading) effective mode changes with time [Fig. 5(c)] up to nearly 30 ps. Later on, a closed tetramer and the fifth molecule, which is gradually departing from it, constitute the molecular system, and a very pronounced half-bell-shaped initial segment can be noticed in all of the corresponding 5-ps-averaged kinetic-energy distributions. The prevailing effective modes are swinging oscillations of the monomer and breathing, pleating, and twisting of the tetramer ring. It is these motions that integrally contribute to the aforementioned half-bell-shaped segment of the total kinetic-energy distribution curve [Fig. 4(a)]. It is worth noting that the long-term stable prevalence of the modes is clearly reflected in the peculiar structure of the overlap matrices of the effective-mode vectors, which characterize the dynamics of the cluster in successive 2-ps intervals. By contrast to the aforementioned situations when the matrices were more or less sparse and the governing modes were more or less substantially coupled to each other and change their roles, here the top left 10×10 block of the matrices undergoes quite regular changes with time after 30 ps. In its own block-diagonal structure, the diagonal sub-blocks acquire a progressively smaller dimensionality, so that by 100 ps already eight effective modes can be distinguished as persistently retaining their character and contribution to the overall dynamics.

At the same time, the dissociation consumes a certain portion of the excess energy, and the translational departure of the monomer and tetramer also requires a certain fraction of the kinetic-energy increment to be spent on it. Hence, the subsequent changes within the tetramolecular ring are not as drastic. And it is this dissociation that results in the abrupt drop in the correlation dependence between the number of effective modes and the mean kinetic energy of the cluster [Fig. 4(b)]. This is clearly illustrated by the time dependences of the number of effective modes (Fig. 6). When the cluster dynamics is governed by the energy redistribution among almost all the effective modes, the leading roles being from time to time switched between them, as in the case of W5_3 trajectories, a nearly constant mean number of modes characterizes the cluster dynamics [Fig. 6(a)]. However, when the character of cluster dynamics is abruptly changed, as in the case of W5_4 trajectories, the number of effective modes, which was nearly constant up to the corresponding time moment, gradually drops to the final value, which reflects the origination of smaller subsystems that become nearly independent with time [Fig. 6(b)]. The corresponding change can be followed in more detail at shorter time intervals around the moment when the cluster decay takes place [Fig. 6(c)]. Note that the number of effective modes within short-term intervals is naturally smaller than that within long-term intervals, because (as was illustrated above) the characters of motions continuously transform into each other, so that the leading modes repeatedly

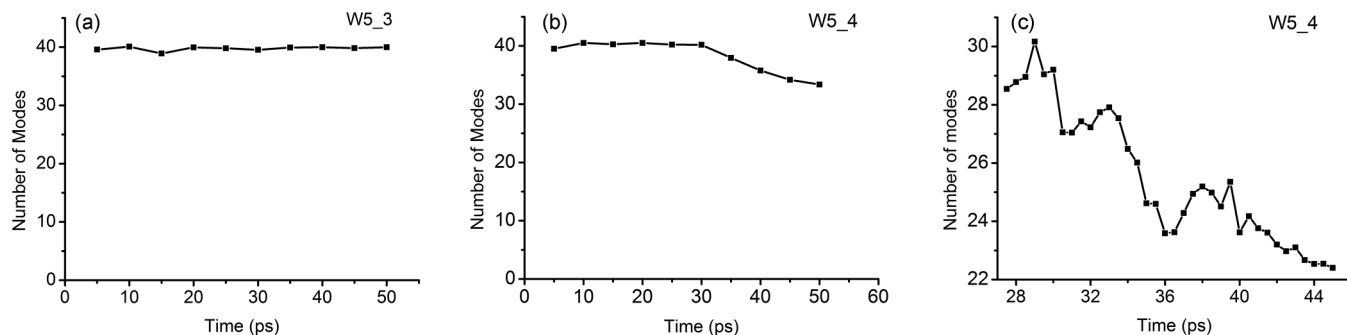


FIG. 6. The numbers of effective modes of a water pentamer within successive short-term intervals along the dynamics trajectories: (a), (b) 5-ps intervals for (a) W5_3 and (b) W5_4 50-ps runs and (c) 0.5-ps intervals for the W5_4 run around and after the cluster decay.

replace each other with time. By 30 ps, the number of effective modes rapidly drops at first to 27 and then below 24 and 23. The drop is nonmonotonous, but rather wavy when a certain energy redistribution over the increasing number of effective modes is followed by a steep drop that corresponds to the short-time accumulation of energy on the smaller number of modes, which makes them process determining within 2- to 3-ps time intervals. This is what results in a drop in the aforementioned integral correlation dependence shown in Fig. 4(b) for the whole W5_4 trajectory when the increase in the total kinetic energy of the system is accompanied by the decrease rather than typical increase in the number of the effective modes of the cluster.

V. CONCLUSIONS

The above analysis shows that the effective-mode approach should by no means be considered as just an auxiliary instrument in vibrational analysis or related statistical description and estimation of the thermodynamic characteristics of the systems of interest. It is an efficient tool of the quantitative analysis of the key processes governing the dynamics of weakly bound systems, particularly clusters stabilized by hydrogen bonds, which are known to provide collective effects reflected in not only correlation between but essentially coupling of the vibrational states of individual molecules. This instrument enables one to quantify the dynamics at femto- to picosecond scales and makes it possible to distinguish the governing kinds of internal dynamics within different time intervals; quantitatively follow the changes in their characters (judged from the overlap matrices) and contributions to the total kinetic energy of the system; analyze particular couplings of normal modes, which approximate the corresponding effective modes; and even suggest criteria that enable one to judge the collectivity of dynamics and the persistency of particular motions, as well as the overall stability of the system or its decomposition into smaller fragments.

In the case of small water clusters considered, at the larger number of molecules in the cluster stabilized by hydrogen bonds, the same weighted activation energy (activation energy per particle) can lead to more noticeable local dynamic changes because of the possibility of the consistent energy redistribution within the cluster. Such redistribution can result in the local temporary accumulation of the kinetic energy on those effective modes that provide the key reorganization of

the structure. This would be impossible in the absence of a hydrogen-bond network between the molecules. Such favorable energy distribution always follows a period when all the molecules in the cluster were hydrogen bonded to each other, being located at quite small O...H distances typical of ordinary or even slightly shortened hydrogen bonds.

An ultimate variant of the reorganization is the dissociation of the cluster system. It is reflected by a drop in the correlation between the number of effective modes and the mean kinetic energy of the system, because a substantial fraction of the excess kinetic energy determines the translational motion of the resulting fragments in opposite directions in space. At the same time, the number of effective modes that provide the dissociation can be judged from the half-bell-shaped first segment of the integral kinetic-energy distribution in the effective modes.

The integral energy distributions can be supplemented with the short-term (≈ 5 or 0.5 ps) distributions that enable one to follow the time dependence of the dynamic changes. Here, the same half-bell-shaped initial segments reflect the strong predominance of particular structure changes predetermined by a few key effective modes. Additionally, the short-term distributions when compared to the integral curve enable one to judge (even without analyzing the structure changes along the trajectory) whether the leading effective modes replace each other during the dynamic evolution or are activated concurrently. In the former case, the short-term curves have clearly descending character, while the integral one involves an extended plateau. In the latter case, the short-term dependences themselves involve a larger or shorter plateau segment.

At the same time, if one turns to the correlation dependence between the number of effective modes and the mean kinetic energy of the cluster, the existence of a plateau segment in it means that the prevailing character of the dynamics is nearly the same despite the increase in the mean kinetic-energy increment. In this situation, the actual dynamics is characterized by larger amplitudes of motions, which nevertheless do not result in drastic changes in the organization of the cluster system. An additional indication of the unchanged character of the dynamics is the close kinetic-energy distribution over the effective modes when nearly the same number of modes provides comparable contributions.

The more extended the plateau in the kinetic-energy distribution over the effective modes the more uniform the

excitation of the larger number of different effective modes; in the case of clusters stabilized by hydrogen bonds, this should be reflected in more or less noticeable consistent changes in the mutual arrangement of molecules, which keep their coordination to the neighbors, and, in this way, provide the survival of the whole bonded structure. The larger the number of molecules in the cluster, the larger the activation energy

that can be redistributed over the effective modes and, thus, accumulated by the unbroken cluster.

ACKNOWLEDGMENT

The work was partly financially supported by the Center for Laser Technology and Material Science.

-
- [1] R. S. Berry and B. M. Smirnov, Phase transitions in various kinds of clusters, *Phys. Usp.* **52**, 137 (2009).
- [2] T. L. Beck, J. Jellinek, and R. S. Berry, Rare gas clusters: Solids, liquids, slush, and magic numbers, *J. Chem. Phys.* **87**, 545 (1987).
- [3] E. D. Belega, D. N. Trubnikov, and L. L. Lohr, Effect of rotation on internal dynamics and phase-space structure of rare-gas trimers, *Phys. Rev. A* **63**, 043203 (2001).
- [4] C. J. Tsai and K. D. Jordan, Theoretical study of small water clusters: Low-energy fused cubic structures for $(\text{H}_2\text{O})_n$, $n = 8, 12, 16$, and 20 , *J. Phys. Chem.* **97**, 5208 (1993).
- [5] U. Buck, I. Ettischer, M. Melzer, V. Buch, and J. Sadlej, Structure and Spectra of Three-Dimensional $(\text{H}_2\text{O})_n$ Clusters, $n = 8, 9, 10$, *Phys. Rev. Lett.* **80**, 2578 (1998).
- [6] J. M. Pedulla and K. D. Jordan, Melting behavior of the $(\text{H}_2\text{O})_6$ and $(\text{H}_2\text{O})_8$ clusters, *Chem. Phys.* **239**, 593 (1998).
- [7] D. J. Wales and M. P. Hodges, Global minima of water clusters $(\text{H}_2\text{O})_n$, $n \leq 21$, described by an empirical potential, *Chem. Phys. Lett.* **286**, 65 (1998).
- [8] H. M. Lee, S. B. Suh, J. Y. Lee, P. Tarakeshwar, and K. S. Kim, Structures, energies, vibrational spectra, and electronic properties of water monomer to decamer, *J. Chem. Phys.* **112**, 9759 (2000).
- [9] H. M. Lee, S. B. Suh, and K. S. Kim, Structures, energies, and vibrational spectra of water undecamer and dodecamer: An ab initio study, *J. Chem. Phys.* **114**, 10749 (2001).
- [10] S. Maheshwary, N. Patel, and N. Sathyamurthy, Structure and stability of water clusters $(\text{H}_2\text{O})_n$, $n = 8-20$: An ab initio investigation, *J. Phys. Chem. A* **105**, 10525 (2001).
- [11] S. D. Belair and J. S. Francisco, Stability of the cubic water octamer, *Phys. Rev. A* **67**, 063206 (2003).
- [12] T. James, D. J. Wales, and J. Hernández-Rojas, Global minima for water clusters $(\text{H}_2\text{O})_n$, $n \leq 21$, described by a five-site empirical potential, *J. Chem. Phys. Lett.* **415**, 302 (2005).
- [13] E. D. Belega, K. A. Tatarenko, D. N. Trubnikov, and E. A. Cheremukhin, The dynamics of water hexamer isomerization, *Russ. J. Phys. Chem. B* **3**, 404 (2009).
- [14] E. D. Belega, D. N. Trubnikov, and E. A. Cheremukhin, Melting of water hexamer, *J. Struct. Chem.* **56**, 52 (2015).
- [15] W. T. C. Cole, J. D. Farrell, D. J. Wales, and R. J. Saykally, Structure and torsional dynamics of the water octamer from THz laser spectroscopy near 215 μm , *Science* **352**, 1194 (2016).
- [16] E. D. Belega, The dynamics of solid and liquid phases of water octamer, decamer, and dodecamer, *Struct. Chem.* **30**, 595 (2019).
- [17] A. Proykova and R. S. Berry, Insights into phase transitions from phase changes of clusters, *J. Phys. B: At. Mol. Opt. Phys.* **39**, R167 (2006).
- [18] R. Lima, Describing the dynamics with a bi-orthogonal decomposition, *Chaos* **2**, 315 (1992).
- [19] P. Holmes, J. L. Lumley, and G. Berkooz, *Turbulence, Coherent Structures, Dynamical Systems and Symmetry* (Cambridge University, Cambridge, England, 1996).
- [20] A. Palacios, G. H. Gunaratne, M. Gorman, and K. A. Robbins, Describing the dynamics with a bi-orthogonal decomposition, *Phys. Rev. E* **57**, 5958 (1998).
- [21] K. Pearson F.R.S., LIII. On lines and planes of closest fit to systems of points in space, *J. Sci. London, Edinburgh Dublin Philos. Mag.* **2**, 559 (1901).
- [22] I. T. Jolliffe, *Principal Component Analysis*, Second Edition, Springer Series in Statistics, (Springer, New York, 2002).
- [23] S. Hayward and N. Go, Collective variable description of native protein dynamics, *Ann. Rev. Phys. Chem.* **46**, 223 (1995).
- [24] M. Karplus and J. N. Kushick, Method for estimating the configurational entropy of macromolecules, *Macromolecules* **14**, 325 (1981).
- [25] R. A. Wheeler, H. Dong, and E. Scott, Quasiharmonic vibrations of water, water dimer, and liquid water from principal component analysis of quantum or QM/MM trajectories, *Chem. Phys. Chem.* **4**, 1227 (2003).
- [26] M. Schmitz and P. Tavan, Vibrational spectra from atomic fluctuations in dynamics simulations. I. Theory, limitations, and a sample application, *J. Chem. Phys.* **121**, 12233 (2004).
- [27] A. Strachan, Normal modes and frequencies from covariances in molecular dynamics or Monte Carlo simulations, *J. Chem. Phys.* **120**, 1 (2004).
- [28] M. Martinez, M.-P. Gaigeot, D. Borgis, and R. Vuilleumier, Extracting effective normal modes from equilibrium dynamics at finite temperature, *J. Chem. Phys.* **125**, 144106 (2006).
- [29] F. Calvo, P. Parneix, and N.-T. Van-Oanh, Finite-temperature infrared spectroscopy of polycyclic aromatic hydrocarbon molecules. II. Principal mode analysis and self-consistent phonons, *J. Chem. Phys.* **133**, 074303 (2010).
- [30] S. E. Brown and V. A. Mandelshtam, Self-consistent phonons: An accurate and practical method to account for anharmonic effects in equilibrium properties of general classical or quantum many-body systems, *Chem. Phys.* **481**, 69 (2016).
- [31] E. D. Belega, A. A. Rybakov, D. N. Trubnikov, and A. I. Chulichkov, Effective dimension of a phase trajectory in the visualization of dynamical systems, *Comput. Math. Math. Phys.* **42**, 1817 (2002).
- [32] E. D. Belega, A. A. Rybakov, D. N. Trubnikov, and A. I. Chulichkov, Modes of movement of rotary trimers of argon atoms, *Khimicheskaya Fizika (Khim. Fiz.)* **23**, 15 (2004) (in Russian).

- [33] A. A. Rybakov, E. D. Belega, and D. N. Trubnikov, Description of nonrigid rotation in small atomic clusters, *Eur. Phys. J. D.* **41**, 297 (2007).
- [34] A. A. Rybakov, E. D. Belega, and D. N. Trubnikov, Effective numbers of modes applied to analysis of internal dynamics of weakly bound clusters, *J. Chem. Phys.* **133**, 144101 (2010).
- [35] P. Pirzadeh, E. N. Beaudoin, and P. G. Kusalik, Structural evolution during water crystallization: Insights from ring analysis, *Chem. Phys. Lett.* **517**, 117 (2011).
- [36] E. D. Belega and D. N. Trubnikov, Modeling of phase transitions in weakly bound molecular clusters, *Doklady Mathematics* **98**, 592 (2018).
- [37] L. D. Landau and E. M. Lifshitz, *Mechanics*, 3rd ed. (Butterworth, Washington, DC, 1976), Vol. 1.
- [38] E. Lambros and F. Paesani, How good are polarizable and flexible models for water: Insights from a many-body perspective, *J. Chem. Phys.* **153**, 060901 (2020).